ARTICLE OPEN

Check for updates

Functional characterization of snoRNA-derived RNA (sdRNA) expression in healthy hematopoiesis and acute myeloid leukemia

Rafael Zinz[1,10], Christian Rohde[1,2,10], Cornelius Pauli[1,2,3,10], Fengbiao Zhou[1,2,10], Azmal Ali Syed[4], Daniel Heid[1,5], Viral Shah[1,2], Niklas Alexander Wahl[1], Adrija Ray[4], Simon Renders[1], Laura Werner[1], Sandra Förmer[1], Carl Ahrens[1], Claudia Baldus[6], Martin Bornhäuser[7], Christoph Röllig[7], Hubert Serve[8], Tim Sauer[1], Jeroen Krijgsveld[4,9], Carsten Müller-Tidow[1,2,9] and Maximilian Felix Blank[1,2,4]✉

© The Author(s) 2026

SnoRNAs are highly expressed in AML and have implications in leukemogenesis and leukemic maintenance. SnoRNAs can be further processed into snoRNA-derived RNAs (sdRNAs). The role of sdRNAs in AML and healthy hematopoiesis remains largely elusive. We characterized sdRNA and snoRNA levels in hematopoietic stem and progenitor cells (HSPCs), healthy WBCs, and 159 intensively treated AML patient samples at initial diagnosis. HSPCs, healthy WBCs, and AML blasts could be differentiated by their sdRNA expression pattern in a cell-type-specific manner. In AML, high sd3′-RNA/snoRNA-host gene ratios were associated with an inverse patient outcome. Particularly, in NPM1-mutated patients with favorable risk stratification and good initial therapy response, high sd3′-RNA ratios identified a subgroup with inferior outcome. High sd3′-RNA ratios were associated with altered oncogenic, inflammatory, and immune response signaling. Forced expression of single sdRNAs, such as sd3′-SNORD78, sd3′-SNORD76, and sd5′-SNORD93, enhanced clonogenic potential in AML and drove sdRNA-specific gene expression signatures in both AML and healthy HSPCs. Exemplarily, we propose and characterize NUDT21, an important regulator of alternative polyadenylation and oncogenic gene expression, as a downstream target of sd3′-SNORD78 in AML. Our data introduce sdRNAs as standalone regulatory effector molecules in healthy hematopoiesis and AML.

Leukemia; https://doi.org/10.1038/s41375-026-03120-z

INTRODUCTION

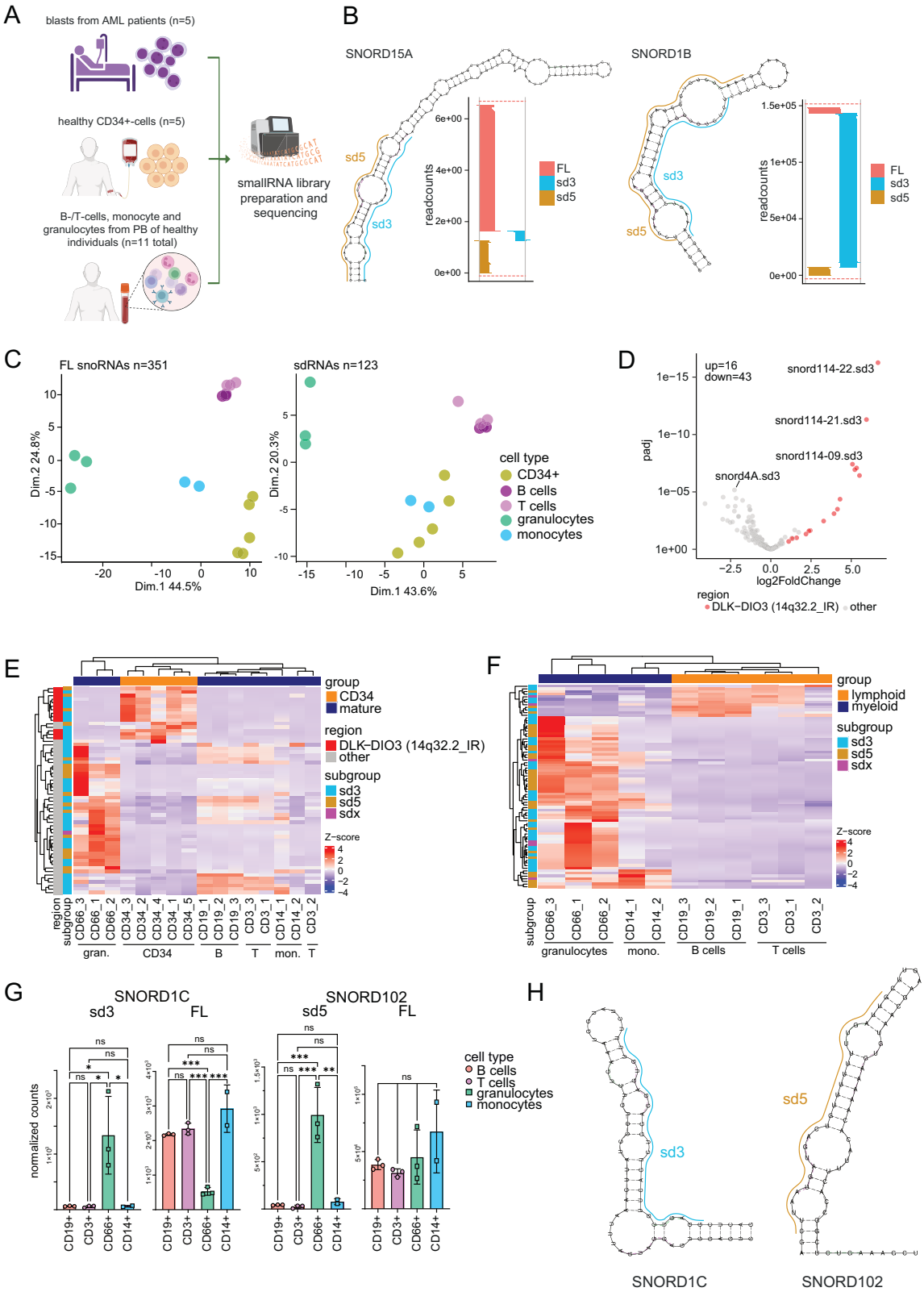
Acute myeloid leukemia (AML) is generally characterized by genomic stability with a rather small number of genetic mutations. Hence, non-genetic plasticity plays an important part in the pathogenesis of AML, which largely involves mechanisms at the transcriptional and post-transcriptional levels. Our group has previously shown that small nucleolar RNAs (snoRNAs) are important players in this regulatory layer in AML. SnoRNAs are small non-coding RNA fragments of 60-300 bases in length that are typically spliced from intronic regions of their respective host genes. Their canonical function is to guide RNA-modifying enzymes to specific ribosomal RNA (rRNA) target sites in a sequence-complementary manner, thereby promoting proper ribosomal biogenesis and function [1]. SnoRNAs are broadly categorized into two major classes: C/D box and H/ACA box snoRNAs. C/D box snoRNAs (SNORDs) associate with fibrillarin, Nop56, Nop58, and 15.5-kDa/Snu13 to form snoRNP complexes that mediate sequence-specific 2′-O-methylation of pre-rRNA. Conversely, H/ACA box snoRNAs (SNORAs) partner with dyskerin, Gar1, Nhp2, and Nop10 to catalyze pseudouridylation of pre-rRNA. If a snoRNA has no reported rRNA modification site, it is classified as an orphan snoRNA.

In acute myeloid leukemia (AML), we previously demonstrated that loss of a single C/D box snoRNA is sufficient to inhibit leukemic cell proliferation [2]. In primary AML blasts, C/D box snoRNAs were specifically enriched in patient samples with high leukemic stem cell (LSC) frequency [3]. Dynamic regulation of 2′-O-methylation at distinct rRNA residues altered translational output and promoted the self-renewal capacity of LSCs [2, 3].

SnoRNAs can be further processed into even smaller fragments, termed snoRNA-derived RNAs (sdRNAs) [4–9]. These sdRNAs can either be derived from the 3′ end (sd3′), the 5′ end (sd5′), or from a central region of the corresponding snoRNA locus (sdx) [6, 10–16]. SdRNA dysregulation has been associated with prostate [17–19],

[1]Department of Medicine V, Hematology, Oncology and Rheumatology, University Hospital Heidelberg, Heidelberg, Germany. [2]Molecular Medicine Partnership Unit (MMPU), University of Heidelberg and European Molecular Biology Laboratory (EMBL), Heidelberg, Germany. [3]Division of Mechanisms Regulating Gene Expression, German Cancer Research Center (DKFZ), Heidelberg, Germany. [4]Division Proteomics of Stem Cells and Cancer, German Cancer Research Center (DKFZ), Heidelberg, Germany. [5]European Molecular Biology Laboratory EMBL, Heidelberg, Germany. [6]Department of Medicine II, Hematology and Oncology, University Hospital of Schleswig-Holstein, Kiel, Germany. [7]Department of Medicine I, University Hospital Carl Gustav Carus, Dresden, Germany. [8]Department of Medicine II, Hematology and Oncology, University Hospital of Frankfurt, Frankfurt (Main), Germany. [9]University of Heidelberg Medical Faculty, Heidelberg, Germany. [10]These authors contributed equally: Rafael Zinz, Christian Rohde, Cornelius Pauli, Fengbiao Zhou. ✉email: maximilianfelix.blank@med.uni-heidelberg.de

Received: 22 December 2025 Revised: 24 July 2026 Accepted: 12 August 2026
Published online: 04 September 2026



breast [20, 21], and pancreatic cancer [22, 23], as well as with cancer immunity [24]. The underlying mechanisms are far from being completely understood, and the role of sdRNAs in AML and healthy hematopoiesis remains unknown.

In this study, we hypothesized that a substantial amount of the implications of snoRNAs in healthy and malignant hematopoiesis could in fact be driven by their corresponding sdRNA product. We aimed to establish sdRNAs as standalone effector

Fig. 1 Cell-type-specific expression signatures of snoRNA-derived RNAs (sdRNAs) in HSPCs and differentiated WBCs. A Small RNA sequencing was performed in five primary AML samples, as well as five CD34$^+$ HSPCs and 11 differentiated WBC samples from healthy donors. Scheme created in BioRender. Rohde, C. (2026) https://BioRender.com/sfdpgiw. **B** Read assignment for sdRNAs and full-length snoRNA expression is exemplarily shown for SNORD15A (left) and SNORD1B (right). Depicted are reads assigned to full-length snoRNAs (sdRNA hostgene, red), 3′-sdRNAs (blue) and 5′-sdRNAs (yellow). The predicted secondary structure of the full-length snoRNA is depicted, the sequences corresponding to 3′-sdRNAs (blue) and 5′-sdRNAs (yellow), as well as box sequences (green/purple) and rRNA complementary region (gray) are highlighted. **C** Principal component analysis (PCA) of FL snoRNA (left) and sdRNA (right) expression in HSPCs and several differentiated WBC populations. **D** Volcano plot showing differential sdRNA expression in CD34$^+$ HSPCs vs. differentiated WBCs. sdRNAs derived from the DLK-DIO3-locus on chromosome 14 are highlighted. **E** Heatmap depicting differentially expressed sdRNAs in CD34$^+$ HSPCs and differentiated WBCs. sdRNAs derived from the DLK-DIO3-locus on chromosome 14 are highlighted. **F** Heatmap comparing sdRNA signatures of myeloid cells (CD66$^+$ granulocytes, CD14$^+$ monocytes) vs. lymphoid cells (CD19$^+$ B-lymphocytes, CD3$^+$ T-lymphocytes). Shown are significantly differentially expressed sdRNAs. **G** Expression of specific sdRNAs in differentiated WBCs is cell-type specific. sd3′-SNORD1C and sd5′-SNORD102 are almost exclusively expressed in granulocytes (CD66$^+$), whereas expression of their host gene is not affected or even lower in granulocytes (CD66$^+$). **H** The predicted secondary structure of SNORD1C and SNORD102 full-length snoRNA is depicted, the sequences corresponding to 3′-sdRNAs (blue) and 5′-sdRNAs (yellow), as well as box sequences (green/purple) and rRNA complementary region (gray) are highlighted.

molecules that act mechanistically independent from their snoRNA host gene and to decipher functional implications of differential sdRNA expression in healthy hematopoiesis and acute myeloid leukemia.

MATERIALS AND METHODS

Cell culture and primary AML/HSPC samples

Cell culture was performed as previously described [25]. Primary AML samples were obtained from bone marrow or peripheral blood of patients with informed consent from the SAL register. The IT1 response (early response assessment ~day21 to first induction) categories are defined as follows: CR: bone marrow blast count <5%; Good response: bone marrow blast count <10%; Moderate response: ≥50% reduction in blast count with residual blast count ≥10%; No response: <50% reduction in blast count. CD34$^+$ HSPCs were isolated from healthy donors at the University Hospital Heidelberg, preparing for allogeneic stem cell transplantation, with informed consent (the study was approved by the Ethics Committee of the Heidelberg Medical Faculty, ethics application number: S-169/2017).

Isolation of primary human blood cells from healthy donors

Mononuclear cells were isolated using density gradient centrifugation with Ficoll-Paque (Miltenyi Biotec) and SepMate™-50 Tubes (StemCell Technologies), according to the manufacturer's instructions. Residual erythrocytes were lysed with RBC Lysis Buffer (ThermoFisher). For population separation, the following Miltenyi MicroBead UltraPure kits were used (human): CD34, CD3, CD14, CD19, and CD66abce. For isolation of CD66abce-positive granulocytes, density gradient centrifugation was omitted.

Generation of knockout cells

Knockouts were generated using the CRISPR-Cas9 system as previously described [25]. For single snoRNA or GAS5 knockout cells, plasmids (GFP +) encoding sgRNAs upstream and downstream of the locus were electroporated (Neon Transfection System) into Kasumi-1 cells. 24–48 h later, GFP-positive cells were sorted into 96-well dishes. Single-cell clones were screened for biallelic target knockout at the DNA and RNA level. SgRNA sequences are indicated in Supplementary table 1.

Expression of snoRNAs/sdRNAs/shRNA

Lentiviral overexpression was performed as previously described [25]. SnoRNA, sdRNA, and shRNA sequences were cloned into the pGreen-puro shRNA vector and expressed from a Pol III promoter (System Biosciences). Small RNA sequences were followed by a terminator sequence (TTTTT). Sequences are indicated in Supplementary table 1.

Colony formation assays

300 cells were seeded into twelve-well plates with 600 µl methylcellulose (04230, STEMCELL Technologies) supplemented with 1% penicillin/streptomycin. After ten days, colonies were counted.

RNA extraction, reverse transcription and quantitative PCR

Total RNA was isolated with the miRNeasy mini kit (Qiagen) and transcribed into cDNA with random hexamers. For sdRNA detection, we used target-specific RT primers for reverse transcription, with an attached sequence for later qPCR amplification to specifically target sdRNAs, but not their full- length snoRNA counterparts. Analysis was done by Real-time PCR (CFX96). Primer sequences are listed in Supplementary table 1.

Steady-state proteome analyses

Steady-state proteome analyses of sd3′-SN78 overexpressing Kasumi-1 cells were performed as previously described [25]. Peptides were analyzed on a Tri-Hybrid Orbitrap Fusion mass spectrometer (Thermo Fisher) operated in DDA mode. All other total proteome analyses were acquired on a timsTOF Pro mass spectrometer (Bruker Daltonics) in DIA (see Supplementary Methods).

Immunoblotting

Cells were lysed, and equal protein amounts were subjected to SDS-PAGE and Western blotting. Primary antibodies anti-NUDT21/CFIM25 (ab183660, abcam) and anti-GAPDH (2118S, CST) were used.

Small RNA sequencing

Libraries were constructed using the NEBNext multiplex small RNA library (E7300S, NEB) according to the instructions of the manufacturer. The barcoded libraries were size-selected using AMPure XP Beads (Beckman Coulter). Sequencing of single-end 75 bp (75SE) was performed on Illumina platforms HiSeq2000 and Nextseq500. For data analysis and sdRNA annotation, see Supplementary Materials.

RNA sequencing

RNAseq libraries were created following the manufacturer's instructions for QuantSeq 3′ mRNA-Seq Library Prep Kit FWD for Illumina (type 015.96, Lexogen Inc), using 2 µg of RNA. See also Supplementary methods.

Bioinformatics

Further bioinformatic analyses were performed using R version 4.4.1 with the R packages specified in Supplementary Table 1. Used ChIP-seq data files from the ENCODE portal [26–29] (https://www.encodeproject.org/) are listed in Supplementary Table 1.

Statistical analysis

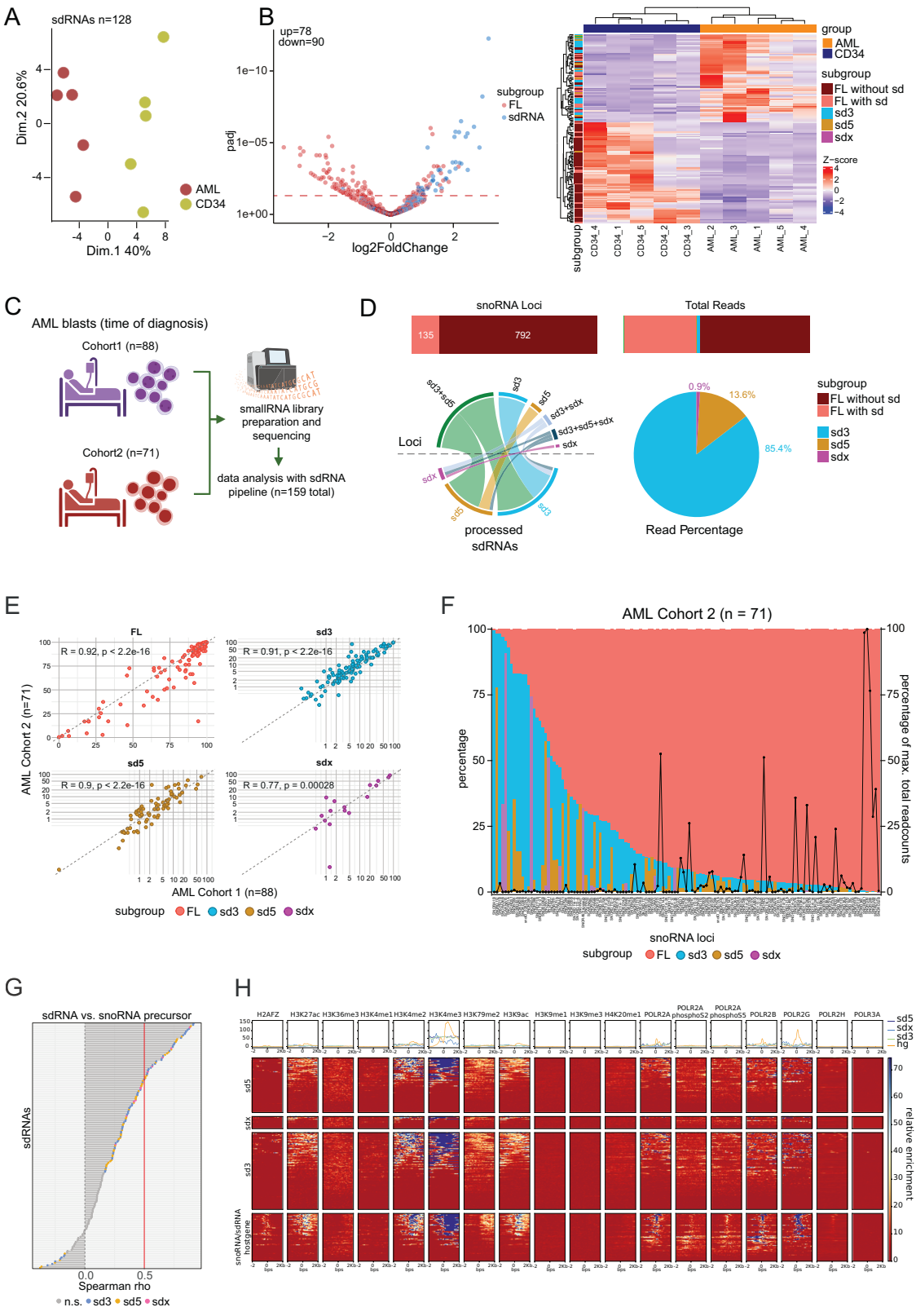
Statistical tests for bar charts and growth assays were performed using R version 4.5 and RStudio version 1.13 or GraphPad Prism version 9.3.1. Values in bar charts and growth assays are presented as mean ± s.d. of replicates. A two-tailed Student's *t* test was used to determine statistical significance for bar charts and growth charts unless stated otherwise.

RNA-RNA interaction in silico prediction

For in silico prediction of RNA-RNA interactions, we used the IntaRNA 2.0 package locally installed [30].

Graphical outlines

Workflow scheme created in BioRender. Rohde, C. (2026) https://BioRender.com/sfdpgiw and https://BioRender.com/yv85j9c.



RESULTS

Cell type-specific expression signatures of snoRNA-derived RNAs (sdRNAs) in HSPCs and differentiated WBCs

To gain insight into sdRNA expression in healthy hematopoiesis, we performed small RNA sequencing in samples from healthy individuals, including hematopoietic stem and progenitor cells (HSPCs, CD34^{+}) ($n = 5$), monocytes ($n = 2$), granulocytes ($n = 3$), T cells ($n = 3$) and B cells ($n = 3$) (Fig. 1A). We assigned reads to full-length snoRNAs if read length was greater than 50 nt and the read start was located within the expected 5′-region. In addition,

Fig. 2 Differential sdRNA expression is a common feature of AML with distinct clustering and processing patterns. A Principal component analysis (PCA) of sdRNA expression in HSPCs ($n = 5$) and primary AML blasts ($n = 5$). **B** Volcano plot (left) and heatmap (right) showing differentially expressed snoRNAs and sdRNAs in AML patient samples as compared to HSPCs (5 vs. 5). Whereas full-length snoRNAs that are not further processed into sdRNAs (FL without sd) were predominantly downregulated in AML, significantly upregulated RNAs in AML were almost exclusively sdRNAs and snoRNAs with derived sdRNAs (FL with sd). **C** Workflow for sdRNA expression analysis in two large AML patient cohorts. RNA was isolated from patient samples at initial diagnosis (ID) before undergoing intensive induction treatment. RNA was subjected to smallRNA library preparation, sequencing, and analysis with our established sdRNA pipeline. Scheme created in BioRender. Rohde, C. (2026) https://BioRender.com/sfdpgiw. **D** Combined analysis of sdRNA processing patterns in both patient cohorts. Upper left: Out of 927 snoRNA loci covered in the smallRNA sequencing data, 135 snoRNAs give rise to sdRNAs (FL with sd). Lower left: Chord plot illustrating the proportion of sdRNA host RNAs giving rise to one or multiple sdRNAs. Upper right: Bar plot representing relative read counts across all patients of snoRNAs (FL with or without sd) and sdRNAs. Lower right: sd3′-RNAs make up more than 85% of sdRNA read counts in AML patient samples. **E** Correlation plot of FL snoRNA and sdRNA expression in both AML patient cohorts, confirming reproducibility across different small RNA sequencing datasets. Indicated is the relative abundance (%) of each RNA type (FL, sd3, sd5, sdx) for each of the respective snoRNA loci. **F** Distribution plot (exemplarily for cohort 2) showing all sdRNA precursor snoRNA loci ($n = 135$) in AML with the amount of full-length snoRNA (FL) and sdRNAs for each snoRNA locus (in %, left y-axis). The black dots indicate total read counts of each snoRNA locus (FL+sdRNA) in relation to the snoRNA locus with the maximum number of reads (right y-axis). **G** Correlation of sdRNA expression and the respective snoRNA host gene. Depicted are Spearman correlation coefficients for each sdRNA and its respective snoRNA host gene based on gene expression data from our small RNA sequencing datasets in primary AML patient samples. sdRNAs with significant (anti)correlation with expression of its host gene are color-coded by sdRNA subtype those without significant (anti)correlation are colored in gray. The red line marks a Spearman correlation coefficient of 0.5. **H** Publicly available ChIP-seq data [26–29] were analyzed for enrichment of polymerases and different promoter marks at snoRNA/sdRNA loci or the respective host gene. A clear enrichment was only observed at the TSS of the respective host gene but not at the snoRNA/sdRNA loci, indicating no independent transcription of snoRNAs/sdRNAs.

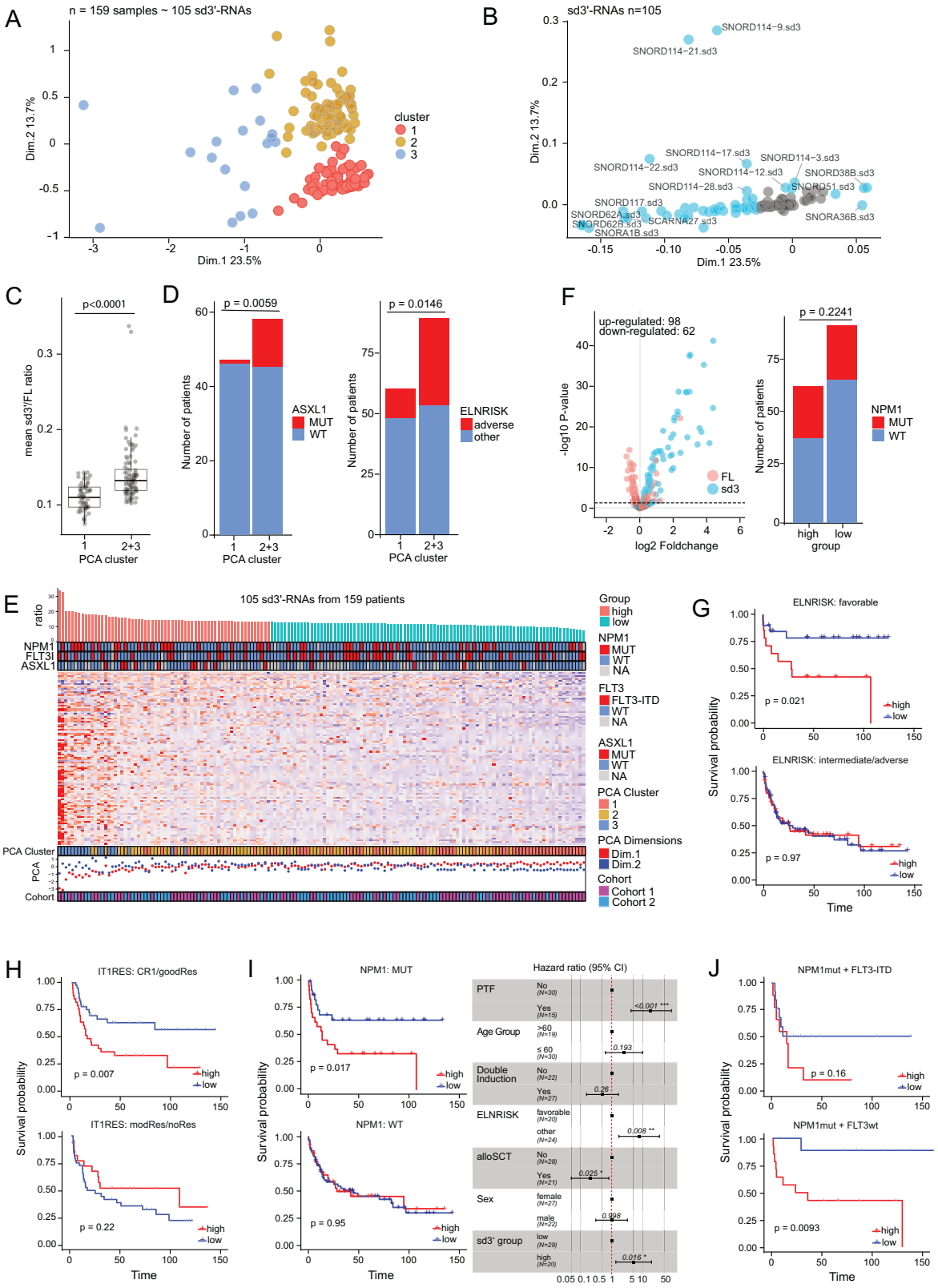
we investigated mapping of shorter reads (15 – 49 nt) to the snoRNA loci (Supplementary Fig. 1A). Most of those reads could be assigned to well-defined regions ranging between 18 and 33 nt in length and corresponded to sdRNAs derived from the 3′-end (sd3′), 5′-end (sd5′), or from a central region of the snoRNA precursor (sdx). Figure 1B exemplifies the snoRNA secondary structure as well as the region assignment method for the SNORD15A and SNORD1B locus. SdRNA start and end positions were highly conserved across all samples, confirming purposeful processing mechanisms and not just random degradation.

A principal component analysis (PCA) using only sdRNA reads resulted in distinct clusters of granulocytes, B-/T-lymphocytes, and monocytes/HSPCs (Fig. 1C), similar to using full-length snoRNA reads. This suggested that sdRNA expression patterns alone can partially distinguish major hematopoietic cell populations. Comparing $CD34^+$ HSPCs and differentiated white blood cells (WBCs), we observed high levels of snoRNAs originating from the DLK-DIO3 locus (chromosome 14) in HSPCs, i.e., the families of SNORD112, SNORD113, and SNORD114, which is in line with previous work [31] (Fig. 1D and Supplementary Fig. 1B–D). These snoRNAs have no known ribosomal RNA methylation target site (orphan snoRNAs) but have been shown to co-facilitate HSC self-renewal [32–35]. Notably, the majority of differentially expressed DLK-DIO3 snoRNAs underwent further processing into sdRNA fragments (Supplementary Fig. 1D), and those accounted for 90% of sdRNAs that were expressed higher in HSPCs compared to mature WBCs (Fig. 1D, E). These findings could suggest that a substantial part of the functional role of DLK-DIO3 snoRNAs—and potentially orphan snoRNAs in general—may actually be driven by their processed sdRNA products.

Comparative analyses of snoRNA and sdRNA expression showed particularly strong differences between WBCs of lymphoid and myeloid lineage (Fig. 1F). We identified several sdRNAs with cell type-specific expression patterns. Exemplarily, sd3′-SNORD1C and sd5′-SNORD102 were almost exclusively expressed in granulocytes ($CD66^+$), while expression of their corresponding FL snoRNAs was either not changed or even reduced relative to the other WBC populations (Fig. 1G). In both cases, the respective sdRNA did not contain the snoRNA/rRNA guide region (Fig. 1H).

SdRNAs are highly expressed in AML with distinct clustering and processing patterns

We performed additional small RNA sequencing on five blast population samples from AML patients at initial diagnosis (see also Fig. 1A). In a PCA including only sdRNA reads, primary AML blasts and $CD34^+$ HSPCs clearly clustered separately (Fig. 2A). Consistent with previous work [31], the majority of full-length snoRNAs had lower expression in AML compared to healthy $CD34^+$ cells (Fig. 2B). The vast majority of those snoRNAs were not processed into sdRNAs (FL without sd). On the sdRNA level, however, we observed elevated expression levels of a large number of sdRNAs in AML as compared to $CD34^+$ cells, while their full-length snoRNA host genes were often unaffected or expressed at lower levels. As representative examples, sd3′-SNORD52 and both SNORD105-derived sdRNAs (sd5′-SNORD105 and sd3′-SNORD105) were highly expressed in AML, while their precursor RNAs (FL with sd) remained unaffected (Supplementary Fig. 2A). This suggested that processing of many snoRNAs was enhanced in AML, with elevated sdRNA ratios as a characteristic feature of AML. These findings prompted us to perform in-depth characterization of sdRNA expression in two large cohorts of AML blasts from intensively treated patients at initial diagnosis, with a total of 159 samples (Fig. 2C and Supplementary Fig. 2B). Already at the read count level, sd3′-RNAs were the most common sdRNA biotype (Fig. 2D and Supplementary Fig. 2C). Out of 927 snoRNA loci with assigned read counts, 135 served as sdRNA host genes. Of these, 72 snoRNAs produced multiple sdRNAs, resulting in a total of 212 distinct sdRNAs. The majority of the sdRNAs originated from the 3′ end (114/212), while the 5′-end-derived sdRNAs accounted for 38.2% (81/212), and only a small fraction (17/212, 8.0%) was derived from the central region of its respective host snoRNA. Although sd3′-RNAs represented 53.8% of the sdRNAs identified, they were significantly overrepresented at the transcript level with 85% of total sdRNA reads across all samples (Fig. 2D and Supplementary Fig. 2D, E). Correlation of snoRNA/sdRNA sequencing data in both AML patient cohorts showed reproducibility and consistency, both serving as quality control and underlining that sdRNA generation is tightly regulated (Fig. 2E and Supplementary Fig. 2C, F, G). The largest relative sdRNA processing occurred in sdRNA host genes with rather low absolute expression levels (Fig. 2F). Notably, ~75% of sdRNAs displayed a correlation coefficient of ≤0.5 with their precursor snoRNA, further supporting that sdRNA production is actively regulated and not a constitutive byproduct of snoRNA expression (Fig. 2G). We assessed publicly available ChIP-sequencing data of polymerases (Pol II/III) and promoter marks [26–29]. We found no enrichment in proximity to the sdRNA/snoRNA loci but at the TSS of the respective host gene (Fig. 2H). This underscores that sdRNAs (and, as is known for the vast majority of snoRNAs) are not independently transcribed but processed from their respective host gene.



Differential sd3′-RNA processing reveals an AML subtype with inverse prognosis within the favorable ELN risk group

Sd3′-RNAs made up the vast majority of sdRNA transcripts. We performed a PCA of sd3′-RNA ratios (sd3′/full-length) across all AML patient samples (Fig. 3A). Samples from both cohorts showed similar and cohort-independent sample distribution after batch effect removal (Supplementary Fig. 3A–D). Notably, this separation was driven by a large number of different sd3′-RNAs and not only a single or few sdRNAs (Fig. 3B). Patients from cluster two and three showed significantly higher mean sd3′-RNA ratios compared to cluster one

Fig. 3 Differential sd3′-RNA processing reveals an AML subtype with inverse prognosis within the favorable ELN risk group. A Principal component analysis (PCA) of sd3′-RNA ratios across 159 primary AML patient samples revealed three distinct clusters. Number of clusters based on elbow method (Supplementary Fig. 3C). **B** Depicted are the correlations between variables and dimensions of the PCA, showing all 3′-sdRNA ratios as the PCA contributors. The top 50 contributors are highlighted. **C** Boxplot showing mean sd3′-RNA ratios across all sd3′-RNA loci for each patient in the different PCA clusters. Clusters 2 and 3 are associated with significantly higher sd3′-RNA ratios. **D** Patients within clusters 2 and 3 (high sd3′-RNA ratios) more commonly have ASXL1 mutations (left) and are more often assigned to the adverse ELN risk group (right). **E** All primary AML samples ($n = 159$) were ranked based on their mean sd3′-RNA ratios across all sd3′-RNA loci and separated into high (sd3′-ratio high) and low (sd3′-ratio low) groups. Heatmap depicting sd3′-RNA ratios for each locus. The mutational status for ASXL1, NPM1 and FLT3-ITD is indicated above. The assignment and contribution to clusters from the PCA (Fig. 3A), as well as the patient cohort, are indicated below. **F** Volcano plot showing differential sd3′-RNA and precursor snoRNA expression in the groups sd3′-ratio high vs. sd3′-ratio low. Right: Sd3′-ratios are not associated with NPM1 mutational status. **G** Patients assigned to the favorable ELN risk group have a significantly poorer overall survival (OS) upon high sd3′-ratio expression. This is not the case for patients in either the intermediate or adverse ELN risk group. Kaplan–Maier plots with survival time in months. **H** Patients with good initial therapy response have a significantly poorer overall survival (OS) upon high sd3′-ratio expression. This is not the case for patients with a poor response to induction therapy. Kaplan–Maier plots with survival time in months. **I** High sd3′-ratios are associated with a significantly poorer overall survival (OS) in patients with NPM1 mutation, but not NPM1 wild-type patients. Kaplan–Maier plot with survival time in months. Multivariate analyses in the subgroup of NPM1-mutated AML (right) show high sd3′-RNA ratios as independent adverse prognostic marker in NPM1-mutated AML. **J** The association of high sd3′-RNA ratios in NPM1-mutated AML was more pronounced in NPM1-mutated with non-concomitant FLT3-aberration. Kaplan–Maier plot with survival time in months.

(Fig. 3C). The higher sd3′-RNA ratios were associated with a higher rate of ASXL1 mutations, adverse ELN risk stratification and reduced patient survival (Fig. 3D and Supplementary Fig. 3E).

This pointed towards an association of high sd3′-RNA ratios with inverse patient outcome. We therefore ranked all primary AML samples based on their mean sd3′-RNA ratios across all loci and separated the samples into two groups (high and low; Fig. 3E). No difference was observed for the rate of NPM1 mutations or FLT3-ITD (Fig. 3F and Supplementary Fig. 3F). All patients were intensively treated (7 + 3 regimens) and groups with high and low sd3′-RNA ratios had similar key patient and intervention characteristics (Supplementary Fig. 3G). Particularly patients assigned to the favorable ELN risk group and patients with good initial therapy response (CR or blast count <10% at day 21) experienced worse overall survival upon high sd3′-RNA ratio expression (Fig. 3G, H). This effect was predominantly driven by the NPM1-mutated subpopulation, as high sd3′-RNA ratios were associated with a significantly worse outcome in patients with NPM1 mutation, but not in NPM1 wild-type patients (Fig. 3I). Multivariate analyses showed high sd3′-RNA ratios as an independent adverse prognostic marker in NPM1-mutated AML (Fig. 3I and Supplementary Fig. 3H–L). The prognostic impact was most pronounced in NPM1-mutant patients without concomitant FLT3-ITD mutation (Fig. 3J).

High sd3′-RNA ratios in NPM1-mutated AML are associated with altered oncogenic and immune response signaling pathways

The negative prognostic impact of high sd3′-RNA ratios was closely linked to the NPM1-mutational status. We next wanted to assess for mechanistic drivers of this NPM1- and sd3′-RNA related phenotype. We selected all NPM1-mutated samples from our merged AML patient cohort ($n = 49$) and stratified them into sd3′-ratio high ($n = 20$) and sd3′-ratio low ($n = 29$) groups (Fig. 4A and Supplementary Fig. 4A, B). We corroborated our analysis by mRNA sequencing data for all NPM1-mutated patient samples (Fig. 4B). Differential expression analysis and subsequent gene set enrichment analysis (GSEA) were performed for both AML patient cohorts separately. High sd3′-RNA ratios were associated with inflammatory and immune response related pathways, including interferon and interleukin signaling (Fig. 4C and Supplementary Fig. 4C). Intracellular signaling pathways closely linked to leukemogenesis, leukemic maintenance and therapeutic escape were enriched in the sd3′-RNA high group, including TNF-alpha signaling via NF-kappa-B, as well as IL6-JAK-STAT3, IL-2-STAT5, and KRAS signaling (Fig. 4D–F and Supplementary Fig. 4D). Pathways involving RNA modification and maturation processes, on the other hand, showed inverse correlation. Comparable enrichment patterns were observed when the aforementioned analyses were performed using high/low stratification based on absolute sd3′-RNA expression levels (Supplementary Fig. 4E, F).

Forced expression of single sdRNAs can enhance clonogenic potential in AML cells

While elevated sd3′-RNA expression was consistently associated with the regulation of distinct signaling pathways across different datasets, this observation remained correlative. We therefore sought to establish whether sdRNAs can directly modulate gene expression and thereby exert causal effects. As an initial approach, we evaluated the phenotypic consequences of perturbing a single sdRNA. Previously, we have shown that depletion of a single snoRNA can significantly reduce cell growth and colony formation capacity in AML [2]. To assess whether this effect could be rescued solely by overexpression of the full-length snoRNA or also by its corresponding sdRNA, we generated snoRNA knockout AML cell lines. As proof-of-principle targets, we chose several sdRNAs from the snoRNA host gene GAS5 (encoding ten C/D box and one H/ACA box snoRNA [18, 36], including the sd3′-RNA of SNORD78, which has been linked to metastatic progression in prostate cancer [18], as well as sd5′-SNORD93, which has previously been linked to increased breast cancer cell invasion [20]. Knockout of SNORD93, the entire GAS5 snoRNA host gene or the GAS5-encoded SNORD78 alone each led to a significant reduction of colony formation capacity but cells were viable, indicating non-essentiality (Fig. 5A and Supplementary Fig. 5A). Forced overexpression of both FL-SNORD93 and sd5′-SNORD93 could rescue the knockout effect and restore colony formation capacity (Fig. 5B). Furthermore, overexpression of FL-SNORD93 and sd5′-SNORD93 in SNORD93$^{+/+}$ control Kasumi-1 cells also enhanced colony formation. For GAS5-encoded snoRNAs, we found significant sdRNA expression in our dataset: sd5′-SNORD44, sd3′-SNORD74, sd3′-SNORD76 and sd3′-SNORD78. Isolated overexpression (Supplementary Fig. 5B) of SNORD74 and its sd3′-RNA did not affect colony growth (Supplementary Fig. 5C), whereas sd5′-SNORD44, sd3′-SNORD76 and both FL-SNORD78 and sd3′-SNORD78 enhanced colony formation capacity (Fig. 5C). We validated these results also in the SNORD78 single-locus knockout cell line and the rescue effect was even stronger for the sdRNA (Fig. 5D). Exemplarily assessed for RNAs derived from the SNORD78 locus, both full-length and sd3′-RNA overexpression enhanced cell proliferation assessed by MTS and cell-growth assays, while cell cycle regulation and apoptosis rates were not significantly affected (Fig. 5E and Supplementary Fig. 5D–F).

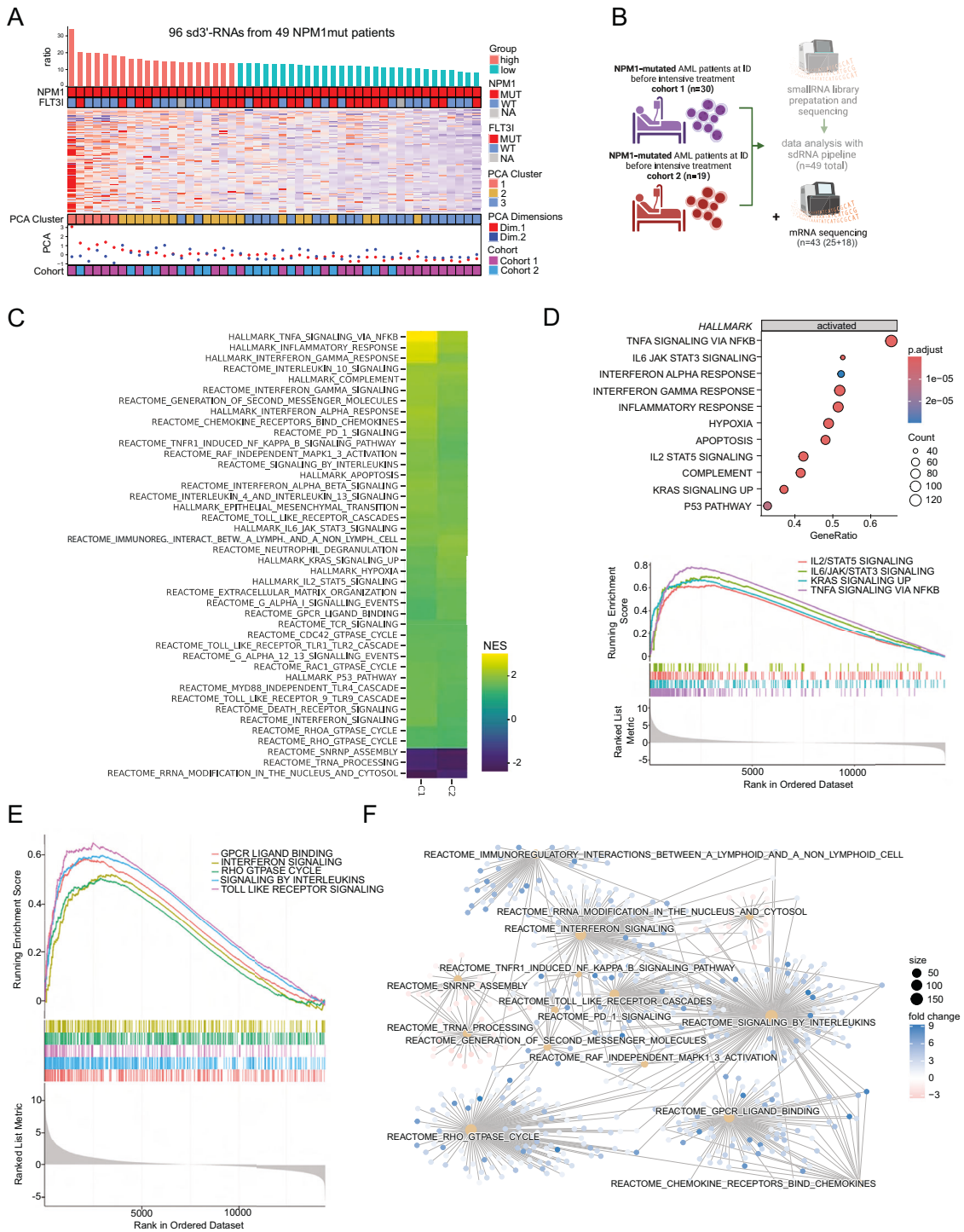
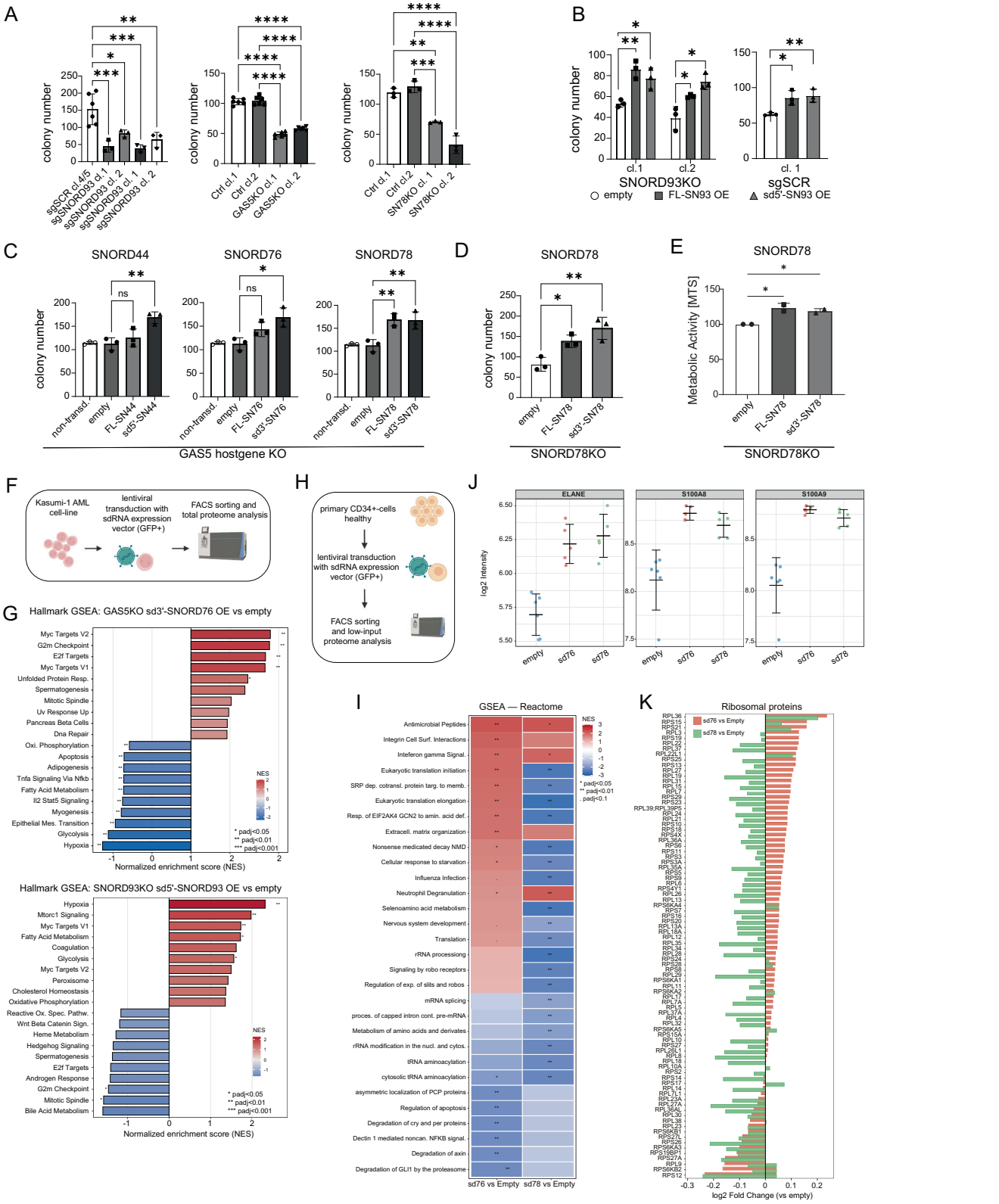


Fig. 4 High sd3′-RNA ratios in NPM1-mutated AML are associated with altered oncogenic and immune response signaling pathways. **A** All NPM1-mutated primary AML samples were ranked based on their median sd3′-RNA ratios across all sd3′-RNA loci and separated in high (sd3′-ratio high) and low (sd3′-ratio low) group. Heatmap depicting sd3′-RNA ratios for each locus. The mutational status for NPM1 and FLT3-ITD is indicated above. The assignment and contribution to clusters from the PCA (Supplementary Fig. 4A), as well as the patient cohort are indicated below. **B** Schematic workflow depiction: RNA from all NPM1-mutated patient samples from both cohorts were subjected to library preparation and sequencing with focus on mRNAs. Scheme created in BioRender. Rohde, C. (2026) https://BioRender.com/sfdpgiw. **C** Differential expression analysis of mRNA sequencing data, comparing patients with high and low sd3′-RNA levels based on overlapping small RNA sequencing data. Depicted are significantly enriched gene sets overlapping in both cohorts, indicating the normalized enrichment scores (NES). GSEA was performed with REACTOME and HALLMARK gene sets. **D** Selection of enriched HALLMARK gene sets. Pathways of oncogenic, inflammatory and immune response signaling are predominantly associated with high sd3′-ratios in NPM1-mutated AML. **E** GSEA enrichment plots for selected REACTOME gene sets in NPM1-mutated/sd3′-ratio-high patient samples, highlighting affected immune response pathways. **F** Gene concept network analysis of selected, significantly differentially expressed REACTOME gene sets in NPM1-mutated sd3′-RNA high versus low samples with functional implications in inflammatory and immune response signaling.



SdRNAs are standalone effector molecules that drive specific gene expression signatures in both AML and healthy HSPCs

Depletion of a single snoRNAs can have a significant impact on the cellular proteome [2]. This effect is thought to be largely due to alterations in snoRNA-guided ribosomal modifications affecting ribosomal function. SdRNAs, however, often do not contain the respective sequence for base-complementarity-based rRNA interaction and are missing box sequences required for snoRNP

Fig. 5 SdRNAs enhance clonogenic potential in AML cells and drive specific gene expression signatures in AML and healthy HSPCs. **A** Knockout of SNORD93, the snoRNA host gene GAS5 and SNORD78 via CRISPR/Cas9 significantly reduced colony formation capacity. Depicted are means ± SD from CFU assays of triplicates and different single-cell-derived KO clones. **B** Left: Lentiviral rescue overexpression of FL-SNORD93 or sd5′-SNORD93 in SNORD93 KO cells could reinduce colony formation capacity and rescue the phenotype of the knock-out cells. Shown for two different single-cell KO clones (cl.6, cl.16), depicted are means ± SD of triplicates. Right: FL-SNORD93 overexpression or sd5′-SNORD93 overexpression in non-KO cells (Kasumi-1 with scramble-sgRNA) significantly enhanced colony formation capacity. Depicted are means ± SD of triplicates. **C** CFU assays upon rescue overexpression of several GAS5-encoded FL snoRNAs and sdRNAs (SNORD44+sd5′, SNORD76+sd3′, SNORD78+sd3′) in GAS5KO cells. Depicted are means ± SD of triplicates. **D** Rescue overexpression of FL-SNORD78 and sd3′-SNORD78 in SNORD78 KO cells showed enhanced colony formation. **E** MTS proliferation assays of Kasumi-1 SNORD78-KO cells with overexpression of empty vector (control), FL-SNORD78 or sd3′-SNORD78. Shown are two biological replicates ($n = 2$; mean of three technical replicates each) performed on different days. **F** Impact of sd3′-SNORD76 and sd5′-SNORD93 overexpression on gene expression in Kasumi-1 AML cells was analyzed by total proteome analysis, empty vector-transduced cells serving as control. Schematic depiction of workflow created in BioRender. Rohde, C. (2026) https://BioRender.com/yv85j9c. **G** GSEA of differentially expressed genes upon sd3′-SNORD76 and sd5′-SNORD93 overexpression in Kasumi-1 AML cells. **H** Impact of sd3′-SNORD76 and sd3′-SNORD78 overexpression on gene expression in $CD34^+$ HSPCs from healthy donors was analyzed by total proteome analysis, with empty vector- transduced cells serving as control. Schematic depiction of workflow created in BioRender. Rohde, C. (2026) https://BioRender.com/yv85j9c. **I** GSEA of differentially expressed genes upon sd3′-SNORD76 and sd3′-SNORD78 overexpression on gene expression in $CD34^+$ HSPCs. **J** Protein levels (LFQ-based in total proteome analysis) of ELANE, S100A8 and S100A9 upon overexpression of empty vector (control), sd3′-SNORD76 and sd3′-SNORD78 in $CD34^+$ HSPCs. **K** Comparative analysis of the impact of sd3′-SNORD76 or sd3′-SNORD78 overexpression (each vs. empty vector control) on ribosomal protein expression levels in $CD34^+$ HSPCs.

formation. We performed total proteome analysis upon separate overexpression of sd3′-SNORD76 and sd5′-SNORD93 (Fig. 5F and Supplementary Fig. 5G) in AML cells. The forced expression of these short RNA fragments led to profound alterations of distinct pathways at the protein level. Oncogenic and immune response pathways ranked among the most affected gene sets (Fig. 5G). Immune response signaling was particularly strongly affected by overexpression of the 3′-sdRNA, again including TNF-alpha signaling and IL-2-STAT5 signaling.

We also assessed the impact of sd3′-SNORD76 and sd3′-SNORD78 overexpression in $CD34^+$ HSPCs by low-input proteomics (Fig. 5H). Expression of a single sdRNA induced significant alterations in the proteome of HSPCs, again comprising immune response pathways such as interferon gamma signaling (Fig. 5I). Some proteins were equally affected in their expression by both sdRNAs, e.g., ELANE, S100A8 and S100A9, with implications in differentiation regulation (Fig. 5J). The majority of affected pathways, however, differed substantially between the two sdRNAs, as for example seen for the opposing regulatory impact on ribosomal protein expression (Fig. 5K), suggesting an sdRNA- and thus sequence-specific impact on gene expression regulation.

NUDT21 is a downstream target of sd3′-SNORD78 in AML with a link to immune response signaling, stemness, and therapy resistance

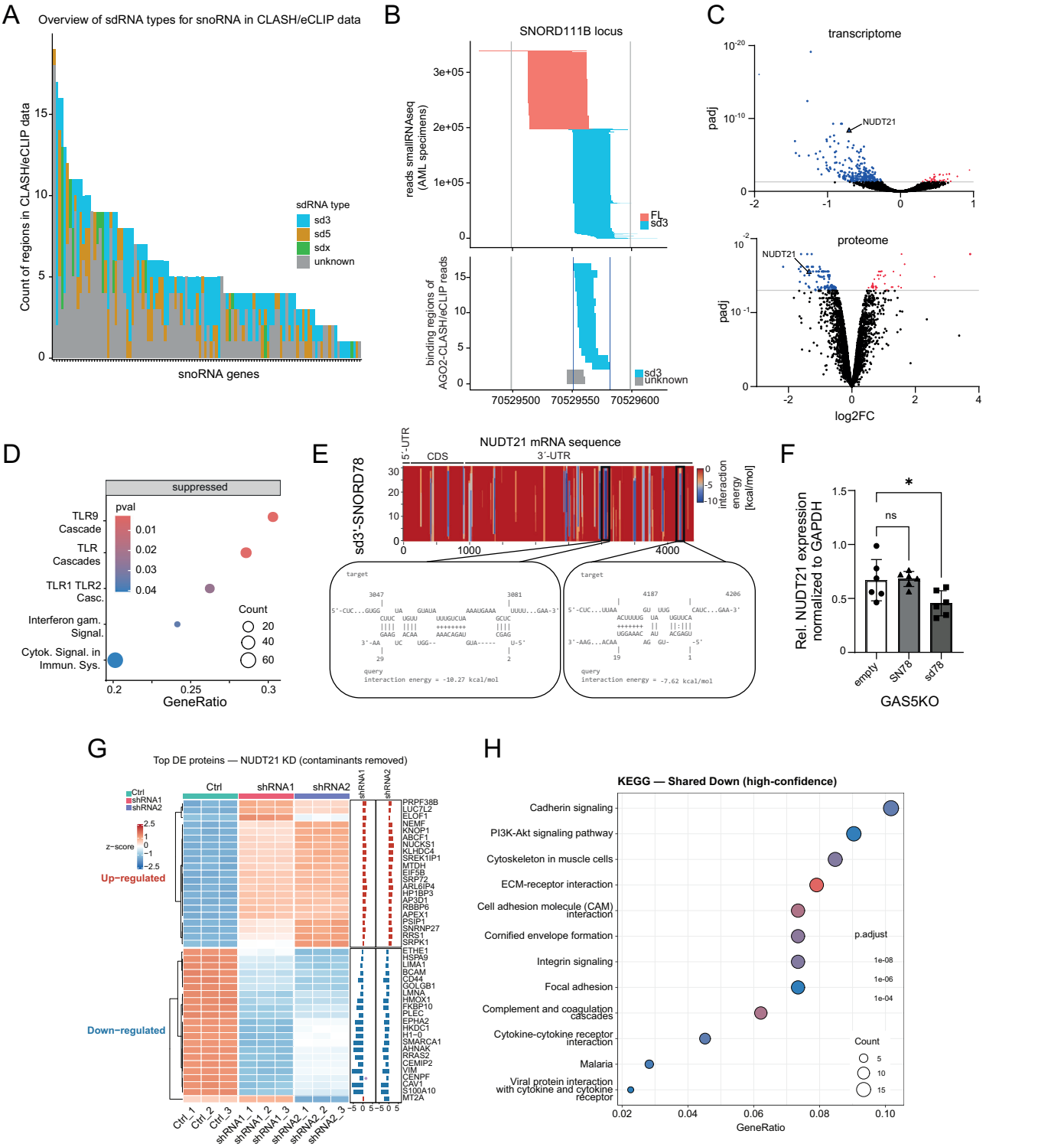
One of the proposed mechanisms of action of sdRNAs is to act in a miRNA-like manner and thus affect the gene expression of complementary target mRNAs [16, 37]. We assessed published AGO2-eCLIP and -CLASH data [38] for snoRNA/sdRNA binding and found numerous reads in these datasets mapping to snoRNA loci. There was a strong sequence overlap with our annotated sdRNA regions, supporting the proposed miRNA-like mode of action (Fig. 6A, B). We chose sd3′-SNORD78 as a proof-of-principle target and performed total proteome and RNA-Seq analysis upon its knockout and rescue expression (Fig. 6C). The majority of affected transcripts and proteins were downregulated. Several inflammation- and immune response-related pathways were negatively affected by sd3′-SNORD78 (Fig. 6D and Supplementary Fig. 6A). Consistently downregulated genes at both the transcript and proteome level included NUDT21 (nudix hydrolase 21) (Fig. 6C and Supplementary Fig. 6B). NUDT21 is part of the 3′-end pre-mRNA polyadenylation and cleavage network with a significant role in alternative polyadenylation (APA) processes [39–41] and is linked to miRNA pathways [42–46]. APA is globally dysregulated across cancer types and has been found to contribute to differentiation blockade in AML [47]. Further, APA is seen as essential for stem cell function across diverse tissues, and recent work showed that varying levels of NUDT21 play an important role in stem cell self-renewal [48]. In both of our pAML datasets, low NUDT21 levels were associated with poor patient outcome, consistent with a negative impact of high sd3′-SNORD78 expression on NUDT21 mRNA levels (Supplementary Fig. 6C). Patients with low NUDT21 mRNA levels had lower CR rates upon intensive induction therapy (Supplementary Fig. 6D). In silico prediction of miRNA-target sites revealed prominent interaction regions between sd3′-SNORD78 and the 3′-UTR of NUDT21 mRNA (Fig. 6E). This suggested that sd3′-SNORD78 directly impacts NUDT21 expression via miRNA-like targeting of its mRNA. We validated the downregulation of NUDT21 upon sd3′-SNORD78 overexpression by RT-qPCR (Fig. 6F).

We characterized the functional significance of the sd3′-SNORD78–NUDT21 axis by NUDT21 knockdown experiments in Kasumi-1 cells coupled with mass spectrometry (Fig. 6G). NUDT21 was sufficiently downregulated with good correlation between the impact of both shRNAs on the proteome, indicating on-target effects (Supplementary Fig. 6E). Consistent with the reported functions of NUDT21, the profound alterations comprised numerous pathways (Supplementary Fig. 6F, G) with known implications in (leukemic) stem cell function and self-renewal, such as PI3K-AKT signaling (Fig. 6H). Further, cell interaction and adhesion pathways, such as cell adhesion molecule (CAM), integrin, and cadherin signaling, were ranked among the most prominently affected gene sets. In AML, those pathways have been closely linked with drug resistance and therapeutic escape in the bone marrow niche [25, 49].

DISCUSSION

Non-coding sequences account for about 98% of the human genome [50], and a large number of non-coding RNAs (ncRNAs) have been linked to oncogenesis or tumor suppression in a variety of different types of cancer. A steadily growing number of studies shed light on the significance of snoRNAs in oncogenesis in general and AML in particular. Their processing into snoRNA-derived fragments added another layer of complexity. This also led to the question of to what extent the sdRNAs constitute the actual effector molecules responsible for the observed pro-oncogenic snoRNA phenotype.

In our study, sdRNAs were clearly defined in sequence and length, specific to the respective locus. Only a fraction of snoRNAs showed relevant processing into sdRNAs, and sdRNA ratios varied greatly between different cell types. Correlation of sdRNA expression with its host snoRNA was often poor. These findings strongly suggest an active and dynamic mechanism underlying snoRNA processing, rather than sdRNAs being spliced at a fixed rate from their host snoRNA. Differential sdRNA expression patterns in HSPCs and WBCs indicate the activation of lineage-specific processing



mechanisms. In leukemogenesis, however, alternative processing mechanisms might be activated, leading to an altered sdRNA signature and downstream gene expression pattern. Consistently, the negative prognostic implications of high sd3′-RNA ratios in NPM1-mutated AML were clearly linked with alterations in oncogenic, inflammatory, and immune response signaling. This connection was not mere correlation, but we established that sdRNAs are stand-alone effector molecules actively impacting cellular phenotypes and gene expression, presumably in a miRNA-like manner. Overexpression of a single sdRNA induced sdRNA-specific proteomic alterations in both AML cell lines and in primary cells (HSPCs), consistently affecting pathways with implications in immune response, oncogenesis, or inflammation. Notably, our functional studies were based on the overexpression of a single sdRNA in vitro, whereas our sequencing datasets revealed coordinated differential expression of numerous sdRNAs. The observed effects therefore likely represent only a subset of the broader changes driven by collective sdRNA activity in vivo.

Fig. 6 NUDT21 is a downstream target of sd3′-SNORD78 in AML with a link to immune response signaling, stemness, and therapy resistance. A Previously published AGO2-eCLIP/CLASH [38] was assessed for snoRNA/sdRNA binding. The diagram shows the number of reads mapping to snoRNA loci. If the respective read overlapped with our annotated sdRNA loci it is color-coded by the sdRNA subtype. In case of no fitting overlap it is colored in gray. **B** Upper: FL snoRNA and 3′-sdRNA annotation in our small RNA sequencing cohort in primary AML specimens. Lower: all reads from the AGO2-eCLIP/CLASH experiment mapping to the SNORD111B locus, the vast majority representing sd3′-SNORD111B reads. **C** Differential expression analysis of mRNA sequencing (upper) and total proteome analysis (lower) for sd3′-SNORD78 versus empty vector overexpression in GAS5 knockout cells. NUDT21 is highlighted in red. **D** GSEA based on mRNA sequencing data from sd3′-SNORD78 versus empty vector overexpression in GAS5 knockout cells. Overexpression of sd3′-SNORD78 associated with significant downregulation of several inflammatory and immune response signaling pathways. **E** In-silico prediction of miRNA-target sites reveals bona fide interacting regions between sd3′-SNORD78 and the 3′-UTR of NUDT21 mRNA with low interaction energy (upper). Exemplary complementary positions are shown with connecting lines between target (NUDT21) and query (sd3′-SNORD78) sequence (lower). **F** Downregulation of NUDT21 mRNA upon sd3′-SNORD78 overexpression in GAS5KO cells was confirmed by RT-qPCR. **G** Heatmap showing the top differentially expressed genes analyzed by total proteomics upon NUDT21 knockdown with two separate shRNAs. **H** GSEA of differentially expressed gene sets (KEGG) upon NUDT21 knockdown (shared in both shRNA experiments).

Forced expression of a single sdRNA could significantly enhance colony formation and cell growth in AML cell lines, often with equal or stronger intensity compared to the respective full-length snoRNA. This could suggest that numerous snoRNA-linked implications in oncogenesis could to a large part, in fact, be mediated by their corresponding sdRNA fragments.

As proof-of-principle sdRNA, we provide evidence that sd3′-SNORD78 negatively regulates NUDT21 expression in a miRNA-like manner. Sd3′-SNORD78 may thus contribute to the fine-tuning of NUDT21 expression and downstream alternative polyadenylation (APA) activity, thereby influencing self-renewal, differentiation, and niche-mediated therapy resistance. NUDT21 is a suspected tumor suppressor in multiple cancer entities [51–55]. The negative regulation of a tumor suppressor could thus constitute a well-fitting mechanism by which pro-oncogenic sdRNAs promote their function. As sd3′-SNORD78 expression has previously also been linked to metastasizing prostate cancer [17, 18], the findings of this study might translate to other cancer entities.

Our data introduce sdRNAs as stand-alone effector molecules in healthy hematopoiesis and acute myeloid leukemia with mechanistic, diagnostic, prognostic, and potentially therapeutic implications.

DATA AVAILABILITY

Sequencing data that support the findings of this study have been deposited in the Gene Expression Omnibus (GEO) under the following accession codes: smallRNA_AML_Cohort: GSE312977, smallRNA_AML_Cohort1_replicates_AND_normal_cells: GSE312978, smallRNA_AML_Cohort2: GSE312979, mRNA_AML_Cohort2: GSE312976. Differential expression analysis from total proteome and RNA-seq experiments has been provided in Supplementary Table 2. All other data supporting the findings of this study are available from the corresponding author on request.

REFERENCES

1. Kiss T. Small nucleolar RNAs: an abundant group of noncoding RNAs with diverse cellular functions. Cell. 2002;109:145–8.
2. Pauli C, Liu Y, Rohde C, Cui C, Fijalkowska D, Gerloff D, et al. Site-specific methylation of 18S ribosomal RNA by SNORD42A is required for acute myeloid leukemia cell proliferation. Blood. 2020;135:2059–70.
3. Zhou F, Liu Y, Rohde C, Pauli C, Gerloff D, Köhn M, et al. AML1-ETO requires enhanced C/D box snoRNA/RNP formation to induce self-renewal and leukaemia. Nat Cell Biol. 2017;19:844–55.
4. Ender C, Krek A, Friedländer MR, Beitzinger M, Weinmann L, Chen W, et al. A human snoRNA with microRNA-like functions. Mol cell. 2008;32:519–28.
5. Kawaji H, Nakamura M, Takahashi Y, Sandelin A, Katayama S, Fukuda S, et al. Hidden layers of human small RNAs. BMC Genomics. 2008;9:157.
6. Taft RJ, Glazov EA, Lassmann T, Hayashizaki Y, Carninci P, Mattick JS. Small RNAs derived from snoRNAs. RNA. 2009;15:1233–40.
7. Brameier M, Herwig A, Reinhardt R, Walter L, Gruber J. Human box C/D snoRNAs with miRNA-like functions: expanding the range of regulatory RNAs. Nucleic Acids Res. 2011;39:675–86.
8. Kishore S, Khanna A, Zhang Z, Hui J, Balwierz PJ, Stefan M, et al. The snoRNA MBII-52 (SNORD 115) is processed into smaller RNAs and regulates alternative splicing. Hum Mol Genet. 2010;19:1153–64.
9. Ono M, Scott MS, Yamada K, Avolio F, Barton GJ, Lamond AI. Identification of human miRNA precursors that resemble box C/D snoRNAs. Nucleic Acids Res. 2011;39:3879–91.
10. Scott MS, Ono M, Yamada K, Endo A, Barton GJ, Lamond AI. Human box C/D snoRNA processing conservation across multiple cell types. Nucleic Acids Res. 2012;40:3676–88.
11. Falaleeva M, Stamm S. Processing of snoRNAs as a new source of regulatory non-coding RNAs: snoRNA fragments form a new class of functional RNAs. Bioessays. 2013;35:46–54.
12. Langenberger D, Çakir MV, Hoffmann S, Stadler PF. Dicer-processed small RNAs: rules and exceptions. J Exp Zool B Mol Dev Evol. 2013;320:35–46.
13. Shi Y, Shi Q, Shen Q, Zhang Q, Cao X. Dicer-independent snRNA/snoRNA-derived nuclear RNA 3 regulates tumor-associated macrophage function by epigenetically repressing inducible nitric oxide synthase transcription. Cancer Commun. 2021;41:140–53.
14. Godang NL, DeMeis JD, Houserova D, Chaudhary NY, Salter CJ, Xi Y, et al. Global Switch from DICER-dependent MicroRNA to DICER-independent SnoRNA-derived RNA Biogenesis in Malignancy. MicroPubl Biol. 2023.
15. Plewka P, Szczesniak MW, Stepien A, Zywicki M, Pacak A, Colombo M, et al. FUS controls the processing of snoRNAs into smaller RNA fragments that can regulate gene expression. Preprint at https://doi.org/10.1101/409250 2018.
16. Wajahat M, Bracken CP, Orang A. Emerging functions for snoRNAs and snoRNA-derived fragments. Int J Mol Sci. 2021;22:19.
17. Martens-Uzunova ES, Jalava SE, Dits NF, van Leenders GJLH, Møller S, Trapman J, et al. Diagnostic and prognostic signatures from the small non-coding RNA transcriptome in prostate cancer. Oncogene. 2012;31:978–91.
18. Martens-Uzunova ES, Hoogstrate Y, Kalsbeek A, Pigmans B, Vredenbregt-van den Berg M, Dits N, et al. C/D-box snoRNA-derived RNA production is associated with malignant transformation and metastatic progression in prostate cancer. Oncotarget. 2015;6:17430–44.
19. Coley AB, Stahly AN, Kasukurthi MV, Barchie AA, Hutcheson SB, Houserova D, et al. MicroRNA-like snoRNA-derived RNAs (sdRNAs) promote castration-resistant prostate cancer. Cells. 2022;11:1302.
20. Patterson DG, Roberts JT, King VM, Houserova D, Barnhill EC, Crucello A, et al. Human snoRNA-93 is processed into a microRNA-like RNA that promotes breast cancer cell invasion. NPJ Breast Cancer. 2017;3:25.
21. Kärkkäinen E, Heikkinen S, Tengström M, Kosma V-M, Mannermaa A, Hartikainen JM. Expression profiles of small non-coding RNAs in breast cancer tumors characterize clinicopathological features and show prognostic and predictive potential. Sci Rep. 2022;12:22614.
22. Müller S, Raulefs S, Bruns P, Afonso-Grunz F, Plötner A, Thermann R, et al. Next-generation sequencing reveals novel differentially regulated mRNAs, lncRNAs, miRNAs, sdRNAs and a piRNA in pancreatic cancer. Mol Cancer. 2015;14:94.
23. Müller S, Raulefs S, Bruns P, Afonso-Grunz F, Plötner A, Thermann R, et al. Erratum to: next-generation sequencing reveals novel differentially regulated mRNAs, lncRNAs, miRNAs, sdRNAs and a piRNA in pancreatic cancer. Mol Cancer. 2015;14:144.
24. Chow RD, Chen S. Sno-derived RNAs are prevalent molecular markers of cancer immunity. Oncogene. 2018;37:6442–62.
25. Allert C, Waclawiczek A, Zimmermann SMN, Gollner S, Heid D, Janssen M, et al. Protein tyrosine kinase 2b inhibition reverts niche-associated resistance to tyrosine kinase inhibitors in AML. Leukemia. 2022;36:2418–29.
26. An integrated encyclopedia of DNA elements in the human genome. Nature. 2012;489:57–74.
27. Luo Y, Hitz BC, Gabdank I, Hilton JA, Kagda MS, Lam B, et al. New developments on the Encyclopedia of DNA Elements (ENCODE) data portal. Nucleic Acids Res. 2020;48:D882–D9.

28. Hitz BC, Lee J-W, Jolanki O, Kagda MS, Graham K, Sud P, et al. The ENCODE Uniform Analysis Pipelines. bioRxiv. 2023. https://doi.org/10.1101/2023.04.04.535623.
29. Kagda MS, Lam B, Litton C, Small C, Sloan CA, Spragins E, et al. Data navigation on the ENCODE portal. Nat Commun. 2025;16:9592.
30. Mann M, Wright PR, Backofen R. IntaRNA 2.0: enhanced and customizable prediction of RNA–RNA interactions. Nucleic acids Res. 2017;45:W435–W9.
31. Warner WA, Spencer DH, Trissal M, White BS, Helton N, Ley TJ, et al. Expression profiling of snoRNAs in normal hematopoiesis and AML. Blood Adv. 2018;2:151–63.
32. Kothari C, Ouellette G, Labrie Y, Jacob S, Diorio C, Durocher F. Identification of a gene signature for different stages of breast cancer development that could be used for early diagnosis and specific therapy. Oncotarget. 2018;9:37407–20.
33. Liuksiala T, Teittinen KJ, Granberg K, Heinäniemi M, Annala M, Mäki M, et al. Overexpression of SNORD114-3 marks acute promyelocytic leukemia. Leukemia. 2014;28:233–6.
34. Valleron W, Laprevotte E, Gautier EF, Quelen C, Demur C, Delabesse E, et al. Specific small nucleolar RNA expression profiles in acute leukemia. Leukemia. 2012;26:2052–60.
35. Wang H, Zhang Z, Han C, Jiang P, Xu J, Han Y, et al. SNORD113–114 cluster maintains haematopoietic stem cell self-renewal via orchestrating the translation machinery. Nat Cell Biol. 2025;27:246–61.
36. Smith CM, Steitz JA. Classification of gas5 as a multi-small-nucleolar-RNA (snoRNA) host gene and a member of the 5′-terminal oligopyrimidine gene family reveals common features of snoRNA host genes. Mol Cell Biol. 1998;18:6897–909.
37. Martens-Uzunova ES, Olvedy M, Jenster G. Beyond microRNA-novel RNAs derived from small non-coding RNA and their implication in cancer. Cancer Lett. 2013;340:201–11.
38. Hejret V, Varadarajan NM, Klimentova E, Gresova K, Giassa I-C, Vanacova S, et al. Analysis of chimeric reads characterises the diverse targetome of AGO2-mediated regulation. Sci Rep. 2023;13:22895.
39. Martin G, Gruber AR, Keller W, Zavolan M. Genome-wide analysis of pre-mRNA 3′ end processing reveals a decisive role of human cleavage factor I in the regulation of 3′ UTR length. Cell Rep. 2012;1:753–63.
40. Brumbaugh J, Di Stefano B, Wang X, Borkent M, Forouzmand E, Clowers KJ, et al. Nudt21 controls cell fate by connecting alternative polyadenylation to chromatin signaling. Cell. 2018;172:629–31.
41. Xiao S, Gu H, Deng L, Yang X, Qiao D, Zhang X, et al. Relationship between NUDT21-mediated alternative polyadenylation process and tumor. Front Oncol. 2023;13:1052012
42. Tamaddon M, Shokri G, Hosseini Rad SMA, Rad I, Emami Razavi À, Kouhkan F. Involved microRNAs in alternative polyadenylation intervene in breast cancer via regulation of cleavage factor "CFIm25. Sci Rep. 2020;10:11608.
43. Wang H, Hu H, Luo Z, Liu S, Wu W, Zhu M, et al. miR-4454 up-regulated by HPV16 E6/E7 promotes invasion and migration by targeting ABHD2/NUDT21 in cervical cancer. Biosci Rep. 2020;40:9
44. Zeng B, Chen Y, Chen H, Zhao Q, Sun Z, Liu D, et al. Synergistic inhibition of NUDT21 by secretory S100A11 and exosomal miR-487a-5p promotes melanoma oligo- to poly-metastatic progression. Mol Oncol. 2023;17:2743–66.
45. Foroutan Kahangi M, Tavakolpour V, Samiei Mosleh I, Oraee-Yazdani S, Kouhkan F. Involvement of oncomiRs miR-23, miR-24, and miR-27 in the regulation of alternative polyadenylation in glioblastoma via CFIm25 cleavage factor. Metab Brain Dis. 2024;39:1269–81.
46. Khan N, Gupta M, Masamha CP. Characterization and molecular targeting of CFIm25 (NUDT21/CPSF5) mRNA using miRNAs. Faseb J. 2025;39:e70324.
47. Davis AG, Johnson DT, Zheng D, Wang R, Jayne ND, Liu M, et al. Alternative polyadenylation dysregulation contributes to the differentiation block of acute myeloid leukemia. Blood. 2022;139:424–38.
48. Tsopoulidis N, Yagi M, Brumbaugh J, Ito S, López-Soriano V, Morris R, et al. Modulation of Nudt21 levels reveals dose-dependent roles of alternative polyadenylation in tissue regeneration. Nat Commun. 2026;17:2005.
49. Allert C, Müller-Tidow C, Blank MF. The relevance of the hematopoietic niche for therapy resistance in acute myeloid leukemia. Int J Cancer. 2024;154:197–209.
50. Mattick JS. Non-coding RNAs: the architects of eukaryotic complexity. EMBO Rep. 2001;2:986–91.
51. Xiong M, Chen L, Zhou L, Ding Y, Kazobinka G, Chen Z, et al. NUDT21 inhibits bladder cancer progression through ANXA2 and LIMK2 by alternative polyadenylation. Theranostics. 2019;9:7156–67.
52. Wang BJ, Liu DC, Guo QY, Han XW, Bi XM, Wang H, et al. NUDT21 suppresses breast cancer tumorigenesis through regulating CPSF6 expression. Cancer Manag Res. 2020;12:3069–78.
53. Gao CC, Xu QQ, Xiao FJ, Wang H, Wu CT, Wang LS. NUDT21 suppresses the growth of small cell lung cancer by modulating GLS1 splicing. Biochem Biophys Res Commun. 2020;526:431–8.
54. Xing Y, Chen L, Gu H, Yang C, Zhao J, Chen Z, et al. Downregulation of NUDT21 contributes to cervical cancer progression through alternative polyadenylation. Oncogene. 2021;40:2051–64.
55. Liu W, Pang Y, Yu X, Lu D, Yang Y, Meng F, et al. Pan-cancer analysis of NUDT21 and its effect on the proliferation of human head and neck squamous cell carcinoma. Aging. 2024;16:3363–85.

ACKNOWLEDGEMENTS

We thank Stefanie Hofmann from the FACS core facility of the Heidelberg University Hospital for cell sorting. The authors gratefully acknowledge the data storage service SDS@hd supported by the Ministry of Science, Research and the Arts Baden-Württemberg and the German Research Foundation through grant INST 35/1503-1 FUGG. The authors acknowledge support by the state of Baden-Württemberg through bwHPC and the German Research Foundation (DFG) through grant INST 35/1597-1 FUGG. We thankfully acknowledge the ENCODE Consortium and the laboratories of Bradley Bernstein (Broad), Michael Snyder (Stanford), Richard Myers (HAIB), Xiang-Dong Fu (UCSD), and Kevin Struhl (HMS) for generating the ChIP-sequencing datasets used in this study.

AUTHOR CONTRIBUTIONS

RZ, CP, and FZ performed the research and interpreted the data. CRo analyzed and interpreted the data; AAS, DH, VS, NAW, AR, SR, LW, SF, and CA performed the research; CB, MB, CRö, and HS provided patient samples; TS contributed to writing the manuscript; JK and CMT contributed to designing the research, interpreting the data and writing the manuscript; and MFB supervised and designed the research, performed the research, analyzed and interpreted the data, and wrote the manuscript.

FUNDING

MFB and CP have been funded by a fellowship of the DKFZ Clinician Scientist Program, supported by the Dieter Morszeck Foundation. MFB, CP, JK, and CMT disclose funding by the German Research Foundation project number 533056198, SFB 1709. Open Access funding enabled and organized by Projekt DEAL.

COMPETING INTERESTS

The authors declare no competing interests.

ETHICS

The study was approved by the Ethics Committee of the Heidelberg Medical Faculty, ethics application number: S-169/2017. All methods were performed in accordance with the relevant guidelines and regulations.

ADDITIONAL INFORMATION

Supplementary information The online version contains supplementary material available at https://doi.org/10.1038/s41375-026-03120-z.

Correspondence and requests for materials should be addressed to Maximilian Felix Blank.

Reprints and permission information is available at http://www.nature.com/reprints

Publisher's note Springer Nature remains neutral with regard to jurisdictional claims in published maps and institutional affiliations.

Open Access This article is licensed under a Creative Commons Attribution 4.0 International License, which permits use, sharing, adaptation, distribution and reproduction in any medium or format, as long as you give appropriate credit to the original author(s) and the source, provide a link to the Creative Commons licence, and indicate if changes were made. The images or other third party material in this article are included in the article's Creative Commons licence, unless indicated otherwise in a credit line to the material. If material is not included in the article's Creative Commons licence and your intended use is not permitted by statutory regulation or exceeds the permitted use, you will need to obtain permission directly from the copyright holder. To view a copy of this licence, visit http://creativecommons.org/licenses/by/4.0/.

© The Author(s) 2026